

Oral malodorous compound causes caspase-8 and -9 mediated programmed cell death in osteoblasts

I. Aoyama, B. Calenic, T. Imai, H. Ii, K. Yaegaki

Department of Oral Health, The Nippon Dental University, Tokyo, Japan

Aoyama I, Calenic B, Imai T, Ii H, Yaegaki K. Oral malodorous compound causes caspase-8 and -9 mediated programmed cell death in osteoblasts. *J Periodont Res* 2012; 47: 365–373. © 2011 John Wiley & Sons A/S

Background and Objective: Hydrogen sulfide (H₂S) is one of two volatile sulfur compounds that are known to be the main cause of oral malodor; the other is methyl mercaptan. Other known volatiles existing in mouth air do not contribute significantly to oral malodor originating in the oral cavity. Hydrogen sulfide is also known to be an etiological factor in periodontal disease. However, the effects of H₂S on alveolar bone remain unclear. The objectives of this study were to determine the apoptotic effects of H₂S on osteoblasts and to verify the apoptotic molecular pathways.

Material and Methods: A clonal murine calvaria cell line was incubated with 50 ng/mL of H₂S. To detect apoptosis, the cells were analysed by flow cytometry and ELISA. Mitochondrial membrane depolarization was assessed using flow cytometry as well. ELISA was used to evaluate the release of cytochrome *c* into the cytosol and to assess Fas ligand, p53, tumor necrosis factor α , interleukin IL1- α , IL- β , IL-2, IL-4, IL-10, interferon- γ , granulocyte-colony stimulating factor and granulocyte-macrophage colony stimulating factor. Caspase-3, -8 and -9 activities were estimated. Expression of *BAX* and *Bcl-2* was assessed by real-time quantitative RT-PCR. DNA fragmentation was detected by single-cell gel electrophoresis. Fas receptors were evaluated by western blotting.

Results: After H₂S incubation, apoptotic levels increased significantly in a time-dependent manner. Mitochondrial membrane depolarization, the release of cytochrome *c*, p53 and caspase-3, -8 and -9 and DNA fragmentation were all significantly greater. *BAX* gene activity was upregulated, whereas *Bcl-2* remained low. Fas ligand/Fas receptor, tumor necrosis factor α and other cytokines were not increased to a significant degree.

Conclusion: At less-than-pathological concentrations in gingival crevicular fluid, H₂S induces apoptosis in osteoblasts. The molecular mechanisms underlying the apoptotic process include p53, a mitochondrial pathway and caspase-8 activation.

Ken Yaegaki, DDS, PhD, Department of Oral Health, Nippon Dental University, 1-9-20 Fujimi, Chiyoda-ku, Tokyo 102-8159, Japan
Tel: +81 3 3261 8791
Fax: +81 3 3261 8796
e-mail: yaegaki-k@tky.ndu.ac.jp

Key words: apoptosis; halitosis; osteoblast; periodontitis

Accepted for publication October 16, 2011

Volatile sulfur compounds (VSCs), specifically hydrogen sulfide (H₂S) and methyl mercaptan (CH₃SH), have been shown to cause halitosis and also to

correlate with the strength of oral malodor (1). Van den Velde *et al.* (1) demonstrated that H₂S and CH₃SH alone significantly contribute to oral malodor

originating from the oral cavity and that the role of other compounds found in mouth air is insignificant. Indeed, H₂S is always present in both physiological

and oral pathological halitosis (2). Previous studies, variously employing gas chromatography, portable gas chromatography or a chemical procedure, have demonstrated a clear relationship among the concentration of VSCs, periodontal disease and periodontal pathogens (3–11). The few papers that failed to demonstrate this relationship utilized a portable sulfide monitor for detecting H₂S (12,13).

Some VSCs are known to be highly toxic. Hydrogen sulfide inhibits cytochrome *c* oxidase via a mechanism similar to that of hydrogen cyanide; consequently, H₂S causes death by means of cellular asphyxiation (14,15). Volatile sulfur compounds have also been shown to comprise one of the pathogenic factors involved in periodontitis (16). Volatile sulfur compounds, particularly H₂S, induce the differentiation of osteoclasts in alveolar bone (17). Moreover, increased levels of VSCs both strongly suppress the synthesis of collagen and increase collagen degradation in human gingival fibroblasts (18,19). Furthermore, VSCs obstruct the normal functioning of the basement membrane by making the mucosa more permeable to periodontitis-causing agents, such as lipopolysaccharides and prostaglandin E₂ (20). Recent studies have described the activation of apoptosis by H₂S in human gingival soft tissues, such as fibroblasts, keratinocytes and keratinocyte stem cells (21–23).

Alveolar bone loss is one of the key events in the development of periodontitis, resulting in part from increased osteoclast resorption and/or decreased osteoblast formation. Some growth factors and inflammatory cytokines affect the development of both osteoclasts and osteoblasts (24). Tumor necrosis factor α (TNF- α) and interleukin 1 β (IL-1 β) can induce apoptosis in mouse osteoblasts (25). Hydrogen sulfide easily diffuses through the oral mucosa of a gingival crevice model (20) and causes pathological changes of alveolar bone tissues in an *in vivo* rat model (17). *In vitro* studies have shown that it also causes inhibition of osteoblast proliferation (26) and induction of osteoclast differentiation (27). We previously reported

that H₂S causes apoptosis in some oral tissues (21–23). However, as H₂S causes either apoptotic or anti-apoptotic activities in different tissues (28–30), H₂S could have an anti-apoptotic effect on osteoblasts.

The objectives of the present study were to determine whether H₂S causes apoptosis in osteoblasts, as it has been shown to do in other oral tissues (21–23) and, if so, to identify these apoptotic molecular pathways.

Material and methods

Cell culture

The osteoblastic cell line MC3T3-E1, derived from newborn mouse calvaria, was employed in this study (26). The cells were cultured in α -minimum essential medium (Gibco, Grand Island, NY, USA) enriched with 10% fetal bovine serum (Hyclone, Logan, UT, USA) and 5 μ g/mL gentamicin (Gibco) at 37°C in an atmosphere of air containing 5% CO₂. For each independent experiment, 5 \times 10⁵ cells were cultured in 25 cm² flasks and allowed to attach overnight. Before their incubation with H₂S, the cells were placed in fresh medium.

Hydrogen sulfide incubation system

The cells were incubated in enriched medium in a chamber infused at approximately 200 mL/min with a constant flow of humidified air containing 5% CO₂ mixed with 50 ng/mL of H₂S for 24, 36 and 48 h, as described previously (21–23), following the procedures of Yaegaki *et al.* (21). Permeator (Gastec, Kanagawa, Japan) and H₂S permeation tubes (Gastec) were used to produce a 50 ng/mL concentration of H₂S in the test chamber. As a result of diffusion, the H₂S concentration in the medium was measured as 18 ng/mL (0.5 μ M), much lower than that found in gingival crevicular fluids from periodontal gingival tissues (31). Healthier gingiva showed lower concentrations (31), so the concentration of H₂S was less than that found in pathological conditions. Control cultures were incubated in 5% CO₂ and 95% air for 24, 36 and 48 h.

Detection of early apoptosis

Apoptotic and nonapoptotic cells were detected using Guava Nexin PCA (GE Healthcare Bioscience, Tokyo, Japan) flow cytometric analysis. Briefly, the cells were stained with two fluorescent dyes: annexin V and 7-amino actinomycin D (7-AAD). Annexin V binds to phosphatidylserine at the cell surface during the early stages of apoptosis and dyes the apoptotic cells, while 7-AAD penetrates the cell membrane only at the later stages of apoptosis or necrosis and binds to DNA. After H₂S incubation, the cells were washed with phosphate-buffered saline (PBS) solution and trypsinized. Pellet (cells fraction), medium and PBS for washing were collected and then resuspended in cold Guava Nexin buffer at 1 \times 10⁶ cells/mL, followed by staining as described above. The samples were analysed using Guava EasyCyte and Guava CytoSoft software (Guava Technologies, Hayward, CA, USA).

To distinguish clearly between apoptosis and necrosis, the cells were also analysed with Cell Death Detection ELISA Plus (Roche Applied Science, Mannheim, Germany) according to the manufacturer's instructions. This assay quantifies histone-complexed DNA fragments, i.e. mono- and oligonucleosomes, in apoptotic cells. After H₂S treatment, the cells were washed with PBS, trypsinized and pelleted, thus removing DNA originating from necrotic cells in the supernatant. The pellet was resuspended in lysis buffer at a concentration of 5 \times 10⁴ cells/mL. After lysis, the supernatant containing histone-complexed DNA fragments was added to a streptavidin-coated microplate for analysis. Peroxidase-labeled anti-DNA antibody binds to the histone-complexed DNA fragments of nucleosomes. After unbound antibodies had been flushed out, the amount of nucleosome material present was measured as peroxidase activity included in the immune complex. The amount of peroxidase was measured with 2,2'-azino-di[3-ethylbenzthiazolinesulfonate] as a substrate, and the microplate reader (Bio-Rad Benchmark; Bio-Rad Japan, Tokyo, Japan) was set to 405 nm, with a wavelength correction set to 490 nm.

An enrichment factor (EF) showing the specific enrichment of mono- and oligonucleosomes released into the cytoplasm was derived by dividing the absorbance value (AV) of the sample by the AV of the negative control.

Detection of mitochondrial membrane potential

Guava EasyCyte MitoPotential Kit (Guava Technologies) was used to detect depolarization of the mitochondrial membrane potential. This assay employs two fluorescent dyes: 5,5',6,6'-terachloro-1,1',3,3'-tetra ethyl benzimidazole carbocyanine iodide (JC-1), for evaluating the mitochondrial membrane potential changes, and 7-AAD for indicating late-stage apoptotic and necrotic cells. After H₂S exposure, the cells were washed with PBS, trypsinized and centrifuged. They were resuspended in 200 μ L of medium at a final concentration of 5×10^5 cells/mL, followed by the addition of 2 μ L of JC-1 and 2 μ L of 7-AAD. After 30 min incubation at 37°C in air containing 5% CO₂, the cells were analysed by means of flow cytometry (Guava EasyCyte; Guava Technologies).

Detection of cytochrome *c*

Rat/mouse cytochrome *c* immunoassay (R&D Systems, Minneapolis, MN, USA) was used for cytochrome *c* detection. The cells were washed three times with PBS to remove serum components and then permeabilized using PBS containing 0.5% Triton X-100 at a concentration of 1×10^6 cells/mL. Following centrifugation, the supernatant, the cytosolic fraction, was added to the wells together with an enzyme-linked monoclonal antibody specific for cytochrome *c*. After the unbound antibodies were washed out, a substrate solution was added to each well according to the manufacturer's instructions. The color developed in proportion to the amount of cytochrome *c* available in each sample. The optical density was measured using a microplate reader (Bio-Rad Benchmark; Bio-Rad Japan) set to 450 nm, with a wavelength correction set to 540 nm.

Detection of caspase-3, -8 and -9 activity

Specific detection kits were employed for the quantitative assessment of caspase-3, -8 and -9 (Calbiochem, San Diego, CA, USA). The assays involve nontoxic and cell-permeable fluorescent markers that bind irreversibly to activated caspase-3, -8 or -9. Briefly, 300 μ L of each sample, concentrated at 1×10^6 cells/mL, was labeled with 1 μ L of fluorescein isothiocyanate fluorescein-conjugated Asp-Glu-Val-Asp-O-methyl-fluormethylketon for caspase-3, fluorescein-conjugated Ile-Glu(OMe)-Thr-Asp-O-methyl-fluormethylketon for caspase-8 or fluorescein-conjugated Leu-Glu(OMe)-His-Asp-O-methyl-fluormethylketon for caspase-9. After 1 h of incubation at 37°C, the FITC label allowed direct detection of each activated caspase with a fluorescence plate reader (Fluoroskan Ascent FL, Vantaa, Finland). The samples were measured at excitation filter = 485 nm and emission filter = 535 nm.

Detection of p53

The p53 pan ELISA kit (Roche Applied Science) was used to detect the tumor-suppressor protein p53, which triggers both mitochondrial pathways and cell-death ligand/receptor pathways involving caspase-8 (32–36). After H₂S incubation, the cells were washed with PBS, trypsinized, pelleted, and resuspended in lysis buffer at a concentration of 1×10^7 cells/mL. Standards, samples or controls were pipetted into wells precoated with the biotin-labeled capture antibody. The p53-containing sample reacts with captured antibody and peroxidase-labeled detection antibody to form a stable immunocomplex. Subsequent to the washing step, the peroxidase bound in the complex is developed by tetramethylbenzidine as a substrate. Assay results are quantified spectrophotometrically at 450 nm, with a correction wavelength of 690 nm using a microtiter plate reader (Bio-Rad Benchmark; Bio-Rad Japan).

Real-time quantitative RT-PCR

Real-time quantitative RT-PCR was used to analyse the levels of pro-apop-

otic (*BAX*) and anti-apoptotic (*Bcl-2*) gene expression. The cells were seeded in enriched medium in 96-well plates at a concentration of 1×10^5 cells/mL and then incubated with or without 50 ng/mL H₂S for 24, 36 or 48 h. TaqMan Gene Expression Cells-to-CT Kit™ (Ambion®, Austin, TX, USA) was used according to the manufacturer's instructions for all steps from isolation of RNA to RT-PCR. To extract RNA, the cells were washed with PBS and treated with lysis solution containing Dnase I. The lysates were used as a template for the synthesis of cDNA. The RT reaction was carried out for 1 h at 37°C followed by 5 min at 95°C. Real-time quantitative RT-PCR (StepOne-Plus Real-Time PCR System; Applied Biosystems, Foster City, CA, USA) was performed in the following conditions: 2 min at 50°C, 10 min at 95°C, followed by 40 cycles of 15 s at 95°C, and 1 min at 60°C. β -Actin was used as an endogenous control. Each sample was analysed in triplicate. The levels of the relative quantification were calculated by STEPONE Software version 2.0 (StepOne-Plus Real-Time PCR System; Applied Biosystems) using the $2^{-\Delta\Delta C_T}$ method (37).

DNA fragmentation

Single-cell gel electrophoresis (Comet Assay; Trevigen, Gaithersburg, MD, USA) was used to detect genomic DNA fragmentation. This assay exploits the capacity of cleaved DNA fragments to migrate out of the nucleoid under the influence of an electric field. Undamaged DNA migrates more slowly than damaged DNA or remains within the confines of the nucleoid. Viewed under the microscope, the cell is comet shaped, with its head corresponding to the nuclear region and its tail showing the damaged DNA fragments.

The cells were suspended in PBS at a concentration of 1×10^5 cells/mL. After cell lysis was accomplished with the use of a lysis solution, the cells were mixed with agarose gel (LMAgarose; Trevigen) and then placed in an electrophoretic field at a constant voltage of 10 V for 10 min. Following electrophoresis, the cells were stained with the use of SYBR Green (Trevigen).

Cell-image analysis, performed with a fluorescence microscope and imaging software (TriTek CometScore, Sumerduck, VA, USA), assessed the following parameters: tail length; percentage of DNA in the tail; and tail moment. Tail length refers to the distance of damaged DNA migration from the nucleoid; percentage of DNA in the tail refers to the proportion of total DNA present in the tail; and tail moment represents the index of induced DNA damage, indicating both the migration of damaged DNA and the relative amount of DNA in the tail, derived from the percentage of DNA in the comet tail and the tail length.

Detection of Fas, Fas ligand and cytokines

Specific ELISA kits were employed for the detection of human Fas ligand (Mouse Fas ligand/TNFSF6 Immunoassay; R&D Systems) and of various cytokines, as follows: TNF- α , IL1- α , IL- β , IL-2, IL-4, IL-10, interferon- γ (IFN- γ), granulocyte-colony stimulating factor (G-CSF) and granulocyte-macrophage colony stimulating factor (GM-CSF) (Multi-Analyte ELISArray™ Kit; SABiosciences, Frederick, MD, USA). Briefly, to detect Fas ligand, the samples (controls or standards) were pipetted into microwells precoated with monoclonal antibodies specific to each substance. Following incubation, an enzyme-linked polyclonal antibody was added to the wells. In the next step, horseradish peroxidase and then the substrate solution were added to each well. The intensity of the color was measured using a microplate reader set to 450 nm, with a wavelength correction set to 540 nm (Bio-Rad Benchmark; Bio-Rad Japan).

Fas activity was detected using FAS (FL-335): sc-7886 antibody (Santa Cruz Biotechnology, Inc., Santa Cruz, CA, USA), and a previously established western blot technique was employed (26,27).

Statistical analysis

Statistical analysis was performed using unpaired *t*-test. Results from all experiments are presented as the

means \pm SD. Statistical significance was accepted at $p < 0.05$.

Results

Apoptosis induced by hydrogen sulfide

The number of early apoptotic cells increased as a result of H₂S incubation in a time-dependent manner compared with their respective controls (8.74 \pm 3.15 vs. 2.40 \pm 1.32% for 24 h;

22.44 \pm 4.10 vs. 2.81 \pm 1.24% for 36 h; and 21.22 \pm 1.18 vs. 2.68 \pm 1.18% for 48 h, $p < 0.01$ respectively, $n = 5$; Fig. 1A). Late apoptotic and necrotic cells were significantly increased for 36 and 48 h (5.87 \pm 2.37 vs. 1.14 \pm 0.03% for 24 h; 44.97 \pm 10.47 vs. 1.71 \pm 0.64% for 36 h; and 50.61 \pm 9.54 vs. 1.98 \pm 0.63% for 48 h, $p < 0.01$ respectively, $n = 5$; Fig. 1B). Moreover, Cell Death ELISA® assay showed that the enrichment factor, indicating the portion of detected

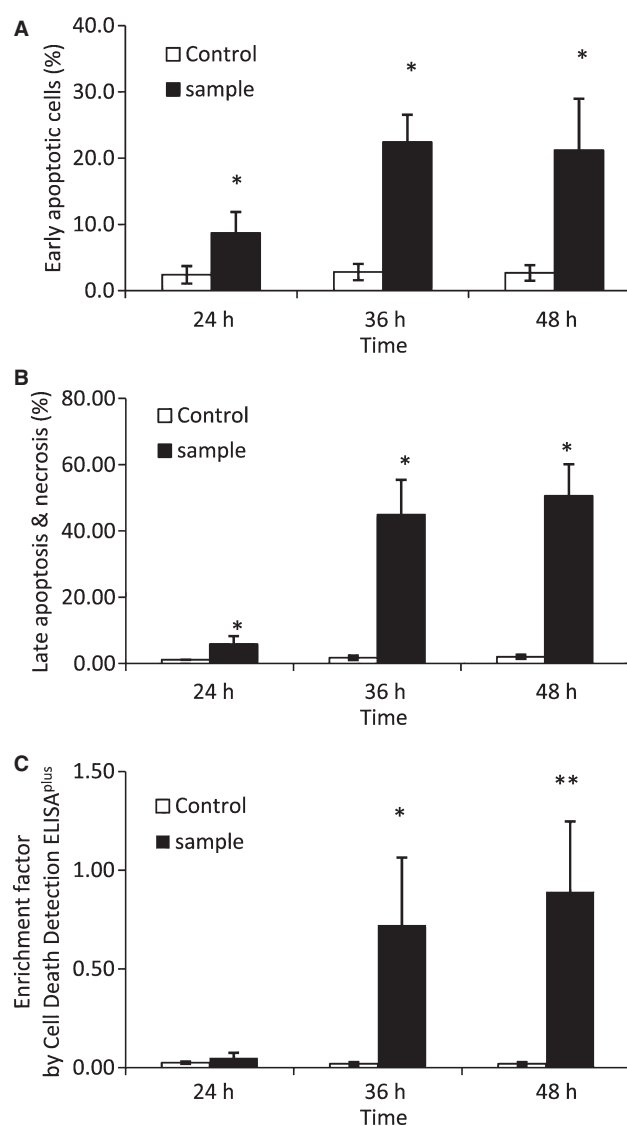


Fig. 1. Detection of early apoptosis, late apoptosis and necrosis. (A) Early apoptotic cells (%) were increased after 24, 36 and 48 h in a time-dependent manner. Each bar represents the mean \pm SD of five independent experiments ($*p < 0.01$). (B) Late apoptotic and necrotic cells were also increased, especially after 36 and 48 h. Each bar represents the mean \pm SD of five independent experiments ($*p < 0.01$). (C) Cell Death ELISA assay also indicated that the apoptotic cells, shown as enrichment factor, were significantly increased in a time-dependent manner. Each bar represents the mean \pm SD of five independent experiments ($**p < 0.05$).

nucleosome in the cytosol of apoptotic cells, increased dramatically compared with controls for 36 and 48 h (0.72 ± 0.34 vs. 0.02 ± 0.01 for 36 h, $p < 0.01$; and 0.89 ± 0.36 vs. 0.02 ± 0.01 for 48 h, $p < 0.05$, $n = 5$; Fig. 1C).

Mitochondrial changes

Membrane depolarization of mitochondria increased at each time point following H₂S incubation (13.86 ± 1.71 vs. $3.69 \pm 1.85\%$ for 24 h; 48.07 ± 5.92 vs. $2.04 \pm 1.53\%$ for 36 h; and 49.12 ± 5.58 vs. $7.17 \pm 2.52\%$ for 48 h, $p < 0.01$ respectively, $n = 5$; Fig. 2A). Cytochrome *c* release into cytosol also increased dramatically compared with controls (1.92 ± 0.50 vs. 0.08 ± 0.01 ng/mL for 24 h, $p < 0.05$; 4.73 ± 0.96 vs. 0.12 ± 0.04 ng/mL for 36 h; and 1.17 ± 0.16 vs. 0.20 ± 0.10 ng/mL for 48 h, $p < 0.01$ for both, $n = 5$; Fig. 2B).

Caspase activities

Caspase-3, -8 and -9 were also strongly activated in H₂S-treated samples com-

pared with their respective controls. Caspase-3, an executioner enzyme of the apoptosis process, was found to be activated significantly more than the control at each time point [8.28 ± 3.03 vs. 1.80 ± 0.65 relative fluorescence units (RFU) for 24 h, $p < 0.05$; 18.54 ± 4.97 vs. 0.41 ± 0.11 RFU for 36 h, $p < 0.01$; and 13.52 ± 4.48 vs. 3.66 ± 1.19 RFU for 48 h, $p < 0.05$, $n = 5$; Fig. 3A]. Caspase-9 activity was significantly higher in the samples than in the control (7.51 ± 3.97 vs. 1.54 ± 0.31 RFU for 24 h, $p < 0.05$; 14.64 ± 3.16 vs. 0.54 ± 0.26 RFU for 36 h; and 14.16 ± 3.61 vs. 1.15 ± 0.73 RFU for 48 h, $p < 0.01$ for both, $n = 5$; Fig. 3B). Caspase-8 activity was also increased in a time-dependent manner, with a significant difference found for 36 and 48 h (1.92 ± 0.63 vs. 1.15 ± 0.44 RFU for 24 h; 6.23 ± 0.82 vs. 0.54 ± 0.13 RFU for 36 h, and 5.19 ± 0.51 vs. 0.65 ± 0.33 RFU for 48 h, $p < 0.01$ for both 36 h and 48 h, $n = 5$; Fig. 3C).

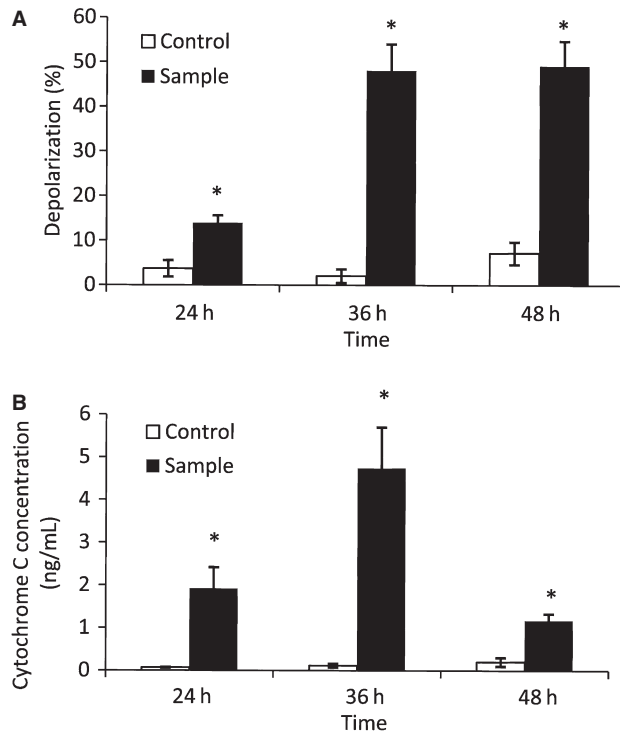


Fig. 2. Mitochondrial changes. (A) Mitochondrial membrane electrical gradient was disrupted after H₂S treatment; the percentage of cells with depolarization increased. Each bar represents the mean \pm SD of five independent experiments ($*p < 0.01$). (B) Cytochrome *c* release into cytosol was also significantly increased, especially after 36 h. Each data point represents the mean \pm SD of five independent experiments ($*p < 0.01$).

p53 expression

The expression of tumor-suppressor protein p53 also increased significantly compared with the controls (48.45 ± 4.76 vs. 15.04 ± 1.44 pg/mL for 24 h; 70.99 ± 5.70 vs. 12.57 ± 2.62 pg/mL for 36 h; and 72.50 ± 6.65 vs. 15.51 ± 3.82 pg/mL for 48 h, $p < 0.01$ respectively, $n = 5$; Fig. 4).

BAX and Bcl-2 gene expression

BAX gene expression became significantly upregulated compared with controls for 36 and 48 h (7.86 ± 0.14 vs. 3.65 ± 0.47 for 36 h; and 4.51 ± 0.04 vs. 3.63 ± 0.06 for 48 h, $p < 0.01$, $n = 5$; Fig. 5A). The anti-apoptotic gene *Bcl-2* remained low following H₂S incubation; no significant difference was found compared with controls (0.57 ± 0.16 vs. 1.02 ± 0.02 for 24 h; 0.79 ± 0.13 vs. 1.31 ± 0.16 for 36 h; and 0.79 ± 0.08 vs. 1.10 ± 0.36 for 48 h, $n = 5$; Fig. 5B).

DNA fragmentation

Tail length, percentage of DNA in tail, and their product, tail moment, are all parameters that increased, indicating significantly more DNA strand breaks in test samples than in corresponding controls (Table 1).

Death ligand pathway

After both 24 and 48 h of H₂S treatment, Fas ligand, Fas receptor, TNF- α , IL1- α , IL- β , IL-2, IL-4, IL-10, IFN- γ , G-CSF and GM-CSF levels remained low, comparable to their respective control groups (data not shown).

Discussion

It has been previously established that the apoptotic process is actively involved in the initiation and development of periodontal diseases (21–23,32). One of the distinguishing characteristics of periodontitis is bone loss. The rate of bone formation and resorption is largely determined by the numbers of osteoblasts and osteoclasts present (24,25). Apoptosis could have a

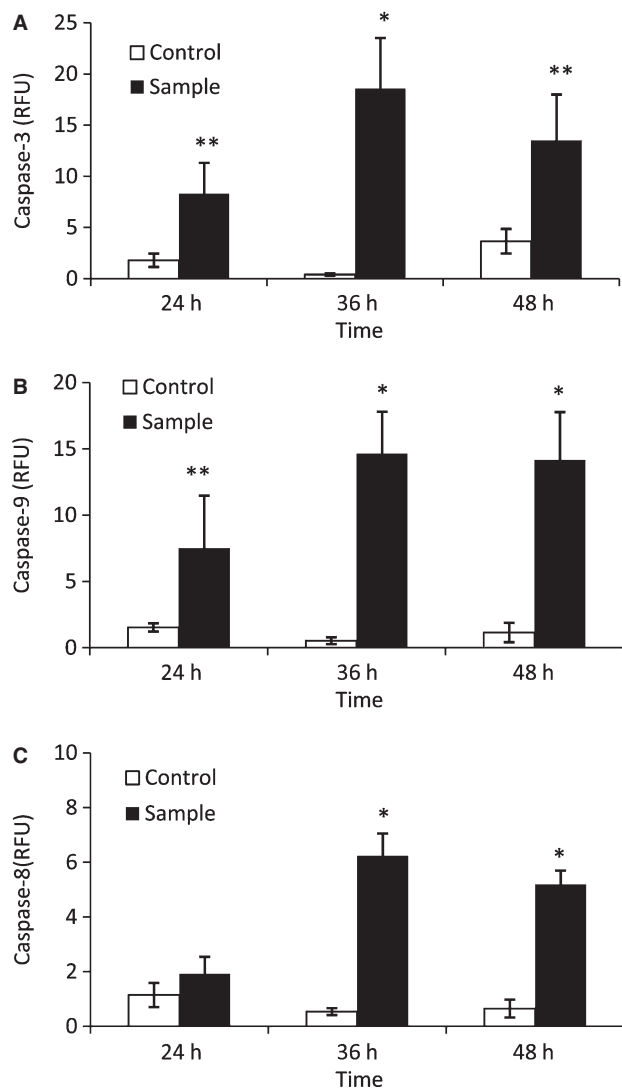


Fig. 3. Detection of caspase-3, -8 and -9 activities. (A) Caspase-3, an executioner caspase, was activated in a time-dependent manner. Each bar represents the mean \pm SD of five independent experiments (* p < 0.01, ** p < 0.05). (B) The activity of caspase-9, an initiator caspase, also increased in a time-dependent manner, suggesting that H₂S-induced apoptosis is activated via an intrinsic apoptotic pathway. Each bar represents the mean \pm SD of five independent experiments (* p < 0.01, ** p < 0.05). (C) Caspase-8 activity also increased in a time-dependent manner. Each bar represents the mean \pm SD of five independent experiments (* p < 0.01).

significant impact on the number of osteoblasts presenting at the site of bone formation. Many reports have suggested that VSCs may accelerate the progression of periodontal disease (20–23,26,27). However, there is limited scientific evidence to explain the relationship between bone resorption and H₂S in periodontitis, although it has been proved that H₂S penetrates into alveolar bone through gingival tissues (17,20). We used 50 ng/mL of H₂S to

simulate its concentration in the tissue in this study, which would approximate the lowest concentration of H₂S present in a gingival crevice or periodontal pocket (31).

In this study, we demonstrate that H₂S, at lower-than-pathological concentrations, induces apoptosis in osteoblasts. After exposure to H₂S, the number of osteoblasts at an early stage of apoptosis was significantly increased. Moreover, late apoptotic and necrotic

cells also increased after H₂S treatment, but flow cytometry cannot distinguish between these two forms of cell death. Therefore, another assay, Cell Death ELISA[®], was employed in this study. A significant increase in the number of apoptotic cells was found in samples exposed to H₂S compared with those not exposed to H₂S after necrotic cells were removed. Both flow cytometry and ELISA showed that H₂S caused apoptosis in osteoblasts.

DNA fragmentation was observed using single-cell gel electrophoresis. The parameters of tail length, percentage of DNA in the tail and tail moment were significantly increased. There is well-documented evidence that the tumor-suppressor protein p53 regulates the cellular response to DNA damage (32). In this study, the total p53 level was significantly increased in H₂S-exposed cells compared with their respective controls. p53 triggers one of the major pathways involved in apoptosis, the cell death ligand/receptor pathway, including caspase-8, and the intrinsic mitochondrial pathway (36).

In the intrinsic pathway, BAX, which is a pro-apoptotic member of the Bcl-2 family, is a p53-primary-response molecule (38). BAX activation mediates mitochondrial membrane depolarization, which can lead to the activation of the mitochondrial apoptotic pathway. Our RT-PCR data demonstrated that the *BAX* gene was upregulated in a time-dependent manner, but *Bcl-2*, an anti-apoptotic gene, remained low. In fact, following H₂S incubation, depolarization of the mitochondrial membrane was significantly increased.

Following membrane depolarization, cytochrome *c* is released from the mitochondrial inner membrane into the cytoplasm (39). In our study, the cytochrome *c* level in the cytoplasm of H₂S-treated cells was significantly higher than in the controls. The release of cytochrome *c* in turn initiates the apoptotic caspase cascade through activation of the initiator, caspase-9. Downstream of the apoptotic cascade is the activation of caspase-3 (40). In the present study, a significant increase in the activity of both caspase-9 and caspase-3 was found after H₂S exposure. We concluded that the intrinsic

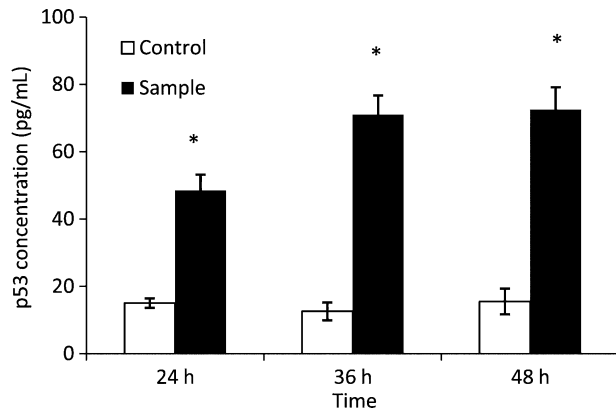


Fig. 4. Effect of H₂S on p53 levels. The expression of tumor-suppressor protein p53 increased in a time-dependent manner. Each data point represents the mean ± SD of five independent experiments (**p* < 0.01).

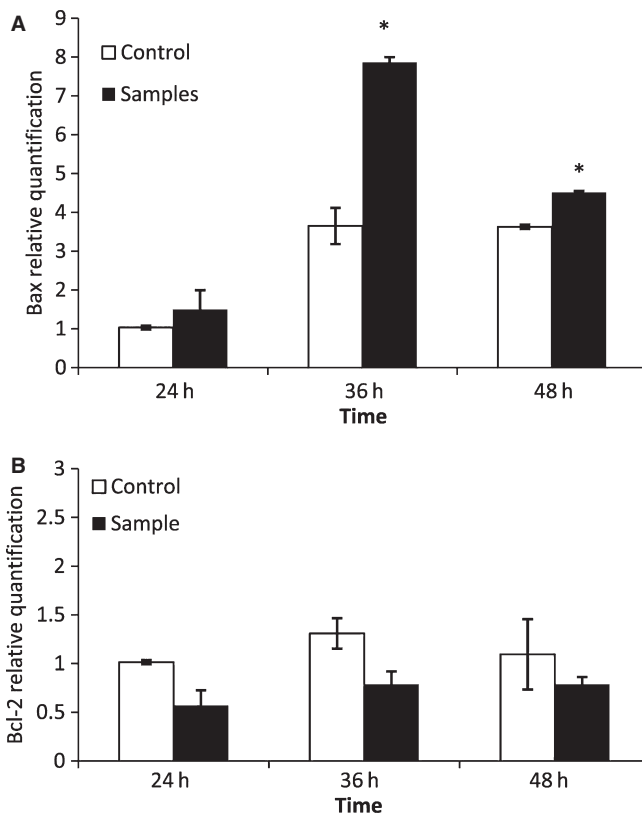


Fig. 5. Real-time quantitative RT-PCR. (A) *BAX* gene activity was upregulated, especially after 36 h. Each bar represents the mean ± SD of five independent experiments (**p* < 0.01). (B) *Bcl-2* gene activity remained low following H₂S treatment.

mitochondrial pathway was activated by H₂S during the process of apoptosis in osteoblasts.

Both caspase-9 and caspase-8 are defined as initiator caspases that can in turn activate caspase-3 as the executor caspase of apoptosis. The extrinsic

pathway, involving a receptor ligand-mediated mechanism, was also examined in this study. Caspase-8 was activated in a time-dependent manner following H₂S incubation. Caspase-8, which is activated by both inducible dimerization and inducible cleavage, is

Table 1. Genomic DNA damage

Group	24 h		36 h		18 h	
	Tail length (pixels)	DNA (%) in tail	Tail length (pixels)	DNA (%) in tail	Tail length (pixels)	Tail moment
Control	2.36 ± 2.28	3.99 ± 3.84	3.41 ± 3.33	4.90 ± 4.83	2.95 ± 2.78	4.76 ± 4.63
Sample	5.85 ± 4.98*	14.16 ± 7.71*	62.62 ± 43.24*	34.06 ± 17.99*	48.22 ± 38.05*	35.01 ± 16.33*
						0.07 ± 0.07
						5.88 ± 5.82*

Tail length is an expression of the distance of DNA damage migration from the nucleoid. DNA (%) in tail is an expression of the proportion of total DNA in tail. Tail moment is the product of the first two parameters, representing the extent of DNA damage. Each data point represents the mean ± SD of five independent experiments; 75 nuclei analysed per experiment (**p* < 0.01).

a key initiator caspase in apoptosis associated with Fas, ligand-activated tumour-necrosis factor receptor-1 or tumour-necrosis factor-related apoptosis-inducing ligands (TRAILs) (34–36,41). Effector cells for TRAILs are T cells or natural killer cells (42,43). However, it is well established that TRAILs cause neither caspase-8 activation nor apoptosis in osteoblasts (44,45); moreover, no T cells or natural killer cells were found in our osteoblast culture. Therefore, caspase-8 activation in this study could not have been caused by TRAILs. Next, we measured Fas and Fas ligand activity. Both levels remained low, suggesting that they are not involved in H₂S-induced apoptosis. Several studies have shown that many cytokines, especially TNF- α , can activate caspase-8 and can initiate apoptosis in osteoblasts (46–55). Thus, we measured the activity of TNF- α , IL1- α , IL- β , IL-2, IL-4, IL-10, IFN- γ , G-CSF and GM-CSF after H₂S exposure. However, there was no difference in these cytokine levels between the test samples and their respective controls.

It has been suggested that none of the cell-death ligand receptors in the extrinsic pathway is involved, while caspase-8 is activated in the apoptotic process. In fact, many previous studies have shown that p53 directly activates the caspase-8 pathway independent of the extrinsic pathways (33–36,56–58). In this study, p53 and caspase-8 were both significantly activated at each time point after H₂S exposure, while no cell-death ligand receptors were activated. This result suggests that caspase-8 activation by H₂S might be directly associated with p53, as described by others (33–36,56–58).

In conclusion, our study determined that H₂S, at concentrations normally found in human gingival crevicular fluid, induces apoptosis in osteoblasts. The molecular mechanisms underlying the apoptotic process include p53, a mitochondrial pathway and caspase-8 activation.

Acknowledgements

This research was supported by Grant-In-Aid No. 20390538 from the Japanese Ministry of Education, Culture,

Sports, Science and Technology, Tokyo, Japan. The osteoblastic cell line MC3T3-E1, derived from newborn mouse calvaria, was a kind gift from Dr H. Sudo of Ohu University, Koriyama, Japan.

References

1. Van den Velde S, van Steenberghe D, Van Hee P, Quirynen M. Detection of odorous compounds in breath. *J Dent Res* 2009;**88**:285–289.
2. Yaegaki K, Sanada K. Volatile sulfur compounds in mouth air from clinically healthy subjects and patients with periodontal disease. *J Periodontol Res* 1992;**27**:233–238.
3. Tanaka M, Yamamoto Y, Kuboniwa M *et al.* Contribution of periodontal pathogens on tongue dorsa analyzed with real-time PCR to oral malodor. *Microbes Infect* 2004;**6**:1078–1083.
4. Kurata H, Awano S, Yoshida A, Ansai T, Takehara T. The prevalence of periodontopathogenic bacteria in saliva is linked to periodontal health status and oral malodour. *J Med Microbiol* 2008;**57**:636–642.
5. Tanaka M, Anguri H, Nonaka A *et al.* Clinical assessment of oral malodor by the electronic nose system. *J Dent Res* 2004;**83**:317–321.
6. Kostelc JG, Zelson PR, Preti G, Tonzetich J. Quantitative differences in volatiles from healthy mouths and mouths with periodontitis. *Clin Chem* 1981;**27**:842–845.
7. Coli JM, Tonzetich J. Characterization of volatile sulphur compounds production at individual gingival crevicular sites in humans. *J Clin Dent* 1992;**3**:97–103.
8. Ratcliff PA, Johnson PW. The relationship between oral malodor, gingivitis, and periodontitis. A review. *J Periodontol* 1999;**70**:485–489.
9. Tsai CC, Chou HH, Wu TL *et al.* The levels of volatile sulfur compounds in mouth air from patients with chronic periodontitis. *J Periodontol Res* 2008;**43**:186–193.
10. Horowitz A, Folke LE. Hydrogen sulfide production in the periodontal environment. *J Periodontol* 1973;**44**:390–395.
11. Morita M, Wang HL. Association between oral malodor and adult periodontitis: a review. *J Clin Periodontol* 2001;**28**:813–819.
12. John M, Vandana KL. Detection and measurement of oral malodour in periodontitis patients. *Indian J Dent Res* 2006;**17**:2–6.
13. Bosy A, Kulkarni GV, Rosenberg M, McCulloch CA. Relationship of oral malodor to periodontitis: evidence of independence in discrete subpopulations. *J Periodontol* 1994;**65**:37–46.
14. Yaegaki K. Oral malodorous compounds are periodontally pathogenic and carcinogenic. *Jpn Dent Sci Rev* 2008;**44**:100–108.
15. Eghbal MA, Pennefather PS, O'Brien PJ. H₂S cytotoxicity mechanism involves reactive oxygen species formation and mitochondrial depolarisation. *Toxicology* 2004;**203**:69–76.
16. Rizzo AA. The possible role of hydrogen sulfide in human periodontal disease. I. Hydrogen sulfide production in periodontal pockets. *Periodontics* 1967;**5**:233–236.
17. Irie K, Ekuni D, Yamamoto T *et al.* A single application of hydrogen sulphide induces a transient osteoclast differentiation with RANKL expression in the rat model. *Arch Oral Biol* 2009;**54**:723–729.
18. Johnson P, Yaegaki K, Tonzetich J. Effect of methyl mercaptan on synthesis and degradation of collagen. *J Periodontol Res* 1996;**31**:323–329.
19. Johnson PW, Yaegaki K, Tonzetich J. Effect of volatile thiol compounds on protein metabolism by human gingival fibroblasts. *J Periodontol Res* 1992;**27**:553–561.
20. Ng W, Tonzetich J. Effect of hydrogen sulfide and methyl mercaptan on the permeability of oral mucosa. *J Dent Res* 1984;**63**:994–997.
21. Yaegaki K, Qian W, Murata T *et al.* Oral malodorous compound causes apoptosis and genomic DNA damage in human gingival fibroblasts. *J Periodontol Res* 2008;**43**:391–399.
22. Calenic B, Yaegaki K, Murata T *et al.* Oral malodorous compound triggers mitochondrial-dependent apoptosis and causes genomic DNA damage in human gingival epithelial cells. *J Periodontol Res* 2010;**45**:31–37.
23. Fujimura M, Calenic B, Yaegaki K *et al.* Oral malodorous compound activates mitochondrial pathway inducing apoptosis in human gingival fibroblasts. *Clin Oral Investig* 2010;**14**:367–373.
24. Jilka RL, Weinstein RS, Bellido T, Parfitt AM, Manolagas SC. Osteoblast programmed cell death (apoptosis): modulation by growth factors and cytokines. *J Bone Miner Res* 1998;**13**:793–802.
25. Yamamoto S, Mogi M, Kinpara K, *et al.* Anti-proliferative capsular-like polysaccharide antigen from *Actinobacillus actinomycetemcomitans* induces apoptotic cell death in mouse osteoblastic MC3T3-E1 cells. *J Dent Res* 1999;**78**:1230–1237.
26. Imai T, Ii H, Yaegaki K, Murata T, Sato T, Kamoda T. Oral malodorous compound inhibits osteoblast proliferation. *J Periodontol* 2009;**80**:2028–2034.
27. Ii H, Imai T, Yaegaki K, Irie K, Ekuni D, Morita M. Oral malodorous compound induces osteoclast differentiation without

- receptor activator of nuclear factor κ B ligand. *J Periodontol* 2010;**81**:1691–1697.
28. Yu YP, Li ZG, Wang DZ, Zhan X, Shao JH. Hydrogen sulfide as an effective and specific novel therapy for acute carbon monoxide poisoning. *Biochem Biophys Res Commun* 2011;**404**:6–9.
 29. Lavu M, Bhushan S, Lefer D. Hydrogen sulfide-mediated cardioprotection: mechanisms and therapeutic potential. *Clin Sci (Lond)* 2010;**120**:219–229.
 30. Shi S, Li QS, Li H *et al.* Anti-apoptotic action of hydrogen sulfide is associated with early JNK inhibition. *Cell Biol Int* 2009;**33**:1095–1101.
 31. Persson S. Hydrogen sulfide and methyl mercaptan in periodontal pockets. *Oral Microbiol Immunol* 1992;**7**:378–379.
 32. Calenic B, Yaegaki K, Kozhuharova A, Imai T. Oral malodorous compound causes oxidative stress and p53-mediated programmed cell death in keratinocyte stem cells. *J Periodontol* 2010;**81**:1317–1323.
 33. Hama-Inaba H, Choi KH, Wang B *et al.* Fas-independent apoptosis induced by UVC in p53-mutated human epithelial tumor A431 cells through activation of caspase-8 and JNK/SAPK. *J Radiat Res (Tokyo)* 2001;**42**:201–215.
 34. Ding HF, McGill G, Rowan S, Schmaltz C, Shimamura A, Fisher DE. Oncogene-dependent regulation of caspase activation by p53 protein in a cell-free system. *J Biol Chem* 1998;**273**:28378–28383.
 35. Ding HF, Lin YL, McGill G *et al.* Essential role for caspase-8 in transcription-independent apoptosis triggered by p53. *J Biol Chem* 2000;**275**:38905–38911.
 36. Haupt S, Berger M, Goldberg Z, Haupt Y. Apoptosis – the p53 network. *J Cell Sci* 2003;**116**:4077–4085.
 37. Livak KJ, Schmittgen TD. Analysis of relative gene expression data using real-time quantitative PCR and the 2^{- $\Delta\Delta C_T$} method. *Methods* 2001;**25**:402–408.
 38. Chipuk JE, Kuwana T, Bouchier-Hayes L *et al.* Direct activation of Bax by p53 mediates mitochondrial membrane permeabilization and apoptosis. *Science* 2004;**303**:1010–1014.
 39. Hearps AC, Burrows J, Connor CE *et al.* Mitochondrial cytochrome *c* release precedes transmembrane depolarisation and caspase-3 activation during ceramide-induced apoptosis of Jurkat T cells. *Apoptosis* 2002;**7**:387–394.
 40. Saunders PA, Cooper JA, Roodell MM *et al.* Quantification of active caspase 3 in apoptotic cells. *Anal Biochem* 2000;**284**:114–124.
 41. Oberst A, Pop C, Tremblay AG *et al.* Inducible dimerization and inducible cleavage reveal a requirement for both processes in caspase-8 activation. *J Biol Chem* 2010;**285**:16632–16642.
 42. Rus V, Nguyen V, Puliaev R *et al.* T cell TRAIL promotes murine lupus by sustaining effector CD4 Th cell numbers and by inhibiting CD8 CTL activity. *J Immunol* 2007;**178**:3962–3972.
 43. Hayakawa Y, Screpanti V, Yagita H *et al.* NK cell TRAIL eliminates immature dendritic cells in vivo and limits dendritic cell vaccination efficacy. *J Immunol* 2004;**172**:123–129.
 44. Atkins GJ, Bourallexis S, Evdokiou A *et al.* Human osteoblasts are resistant to Apo2L/TRAIL-mediated apoptosis. *Bone* 2002;**31**:448–456.
 45. Bu R, Borysenko CW, Li Y *et al.* Expression and function of TNF-family proteins and receptors in human osteoblasts. *Bone* 2003;**33**:760–770.
 46. Son YO, Kook SH, Choi KC *et al.* Quercetin, a bioflavonoid, accelerates TNF-alpha-induced growth inhibition and apoptosis in MC3T3-E1 osteoblastic cells. *Eur J Pharmacol* 2006;**529**:24–32.
 47. Chua CC, Chua BH, Chen Z *et al.* TGF-beta1 inhibits multiple caspases induced by TNF-alpha in murine osteoblastic MC3T3-E1 cells. *Biochim Biophys Acta* 2002;**1593**:1–8.
 48. Suh KS, Koh G, Park CY *et al.* Soybean isoflavones inhibit tumor necrosis factor-alpha-induced apoptosis and the production of interleukin-6 and prostaglandin E2 in osteoblastic cells. *Phytochemistry* 2003;**63**:209–215.
 49. Kim KB, Choi YH, Kim IK *et al.* Potentiation of Fas- and TRAIL-mediated apoptosis by IFN-gamma in A549 lung epithelial cells: enhancement of caspase-8 expression through IFN-response element. *Cytokine* 2002;**20**:283–288.
 50. Hopkins-Donaldson S, Ziegler A, Kurtz S *et al.* Silencing of death receptor and caspase-8 expression in small cell lung carcinoma cell lines and tumors by DNA methylation. *Cell Death Differ* 2003;**10**:356–364.
 51. Shankaranarayanan P, Nigam S. IL-4 induces apoptosis in A549 lung adenocarcinoma cells: evidence for the pivotal role of 15-hydroxyeicosatetraenoic acid binding to activated peroxisome proliferator-activated receptor gamma transcription factor. *J Immunol* 2003;**170**:887–894.
 52. Adachi Y, Taketani S, Ikehara S *et al.* Apoptosis of colorectal adenocarcinoma induced by 5-FU and/or IFN-gamma through caspase 3 and caspase 8. *Int J Oncol* 1999;**15**:1191–1196.
 53. Refaeli Y, Van Parijs L, London CA, Tschopp J, Abbas AK. Biochemical mechanisms of IL-2-regulated Fas-mediated T cell apoptosis. *Immunity* 1998;**8**:615–623.
 54. Thorburn J, Frankel AE, Thorburn A. Apoptosis by leukemia cell-targeted diphtheria toxin occurs via receptor-independent activation of Fas-associated death domain protein. *Clin Cancer Res* 2003;**9**:861–865.
 55. Schmidt-Mende J, Tehrani R, Forsblom AM, Joseph B, Hellström-Lindberg E *et al.* Granulocyte colony-stimulating factor inhibits Fas-triggered apoptosis in bone marrow cells isolated from patients with refractory anemia with ringed sideroblasts. *Leukemia* 2001;**15**:742–751.
 56. Liu JJ, Nilsson A, Oredsson S *et al.* Boswellic acids trigger apoptosis via a pathway dependent on caspase-8 activation but independent on Fas/Fas ligand interaction in colon cancer HT-29 cells. *Carcinogenesis* 2002;**23**:2087–2093.
 57. Jones DT, Ganeshaguru K, Virchis AE *et al.* Caspase 8 activation independent of Fas (CD95/APO-1) signaling may mediate killing of B-chronic lymphocytic leukemia cells by cytotoxic drugs or gamma radiation. *Blood* 2001;**98**:2800–2807.
 58. Schuler M, Green DR. Mechanisms of p53-dependent apoptosis. *Biochem Soc Trans* 2001;**29**:684–688.

This document is a scanned copy of a printed document. No warranty is given about the accuracy of the copy. Users should refer to the original published version of the material.